Arabian Journal of Chemical and Environmental Research

Vol. 13 Issue 1 (2026) 127–142

Kinetics, thermodynamics and antimicrobial activities of Ni(II), Cu(II) AND Zn(II) mixed ligand complexes derived from isatin and isonicotinic acid hydrazide with thiophene

Isaac T. Iorkpiligh[1]*, Grace E. Iniama[2], John U. Ahile[1], Samuel T. Dafa[3] and Elizabeth Angwe[1]

[1]*Department of Chemistry, Benue State University, Makurdi, Nigeria*
[2]*Department of Pure and Applied Chemistry, University of Calabar, Calabar-Nigeria*
[3]*Department of Chemistry, Federal University of Technology Minna, Niger State–Nigeria*

Correspondance email: *mynameisterungwa@gmail.com* ; +2348037228864
Co-authors emails: *geiniama@yahoo.com, ahileuj@gmail.com, dafaterungwa@fuminna.edu.ng, elizabethangwe992@gmail.com*

Received 27 December, 2025, Revised xx January 2026, Accepted xx January 2026

Cited as: Iorkpiligh I.T., Iniama G.E., Ahile J.U., Dafa S.T., Angwe E. (2026). Kinetics, thermodynamics and antimicrobial activities of Ni(II), Cu(II) AND Zn(II) mixed ligand complexes derived from isatin and isonicotinic acid hydrazide with thiophene, Arab. J. Chem. Environ. Res. 13(1), 127-142

Abstract

The Schiff base ligand isatin-isonicotinylhydrazone (ISINH) was synthesized from isatin and isonicotinic acid hydrazide. The ligand was used to prepare the Ni(II), Cu(II) and Zn(II) mixed ligand complexes with thiophene. The melting points of the synthesized compounds were high (195.8–287.6 ^{o}C) while their conductivities were low (0.03–0.10 µs/cm). Infrared spectra studies proved that the ligand is bidendate with oxygen and nitrogen donor atoms. Information from the uv spectra data suggested octahedral geometry for the complexes. Thermodynamic studies showed that the Gibb's free energy (ΔG) of the complexes were: 198.65, 220.43, 204.93 and 177.07kJ/mol. The enthalpy change (ΔH) values were 28.50, 23.40, 37.31 and 21.00 kJ/mol whilethe entropy change (ΔS) were negative (-250.9, -261.6, -241.8 and -23.02 kJ/mol). The kinetic studies showed that the activation energy (Ea) were 34.13, 29.66, 43.07 and 26.63 while the rate constant (k) were 0.4190, 0.6667, 0.5218 and 0.3215 $min^{-1.}$ The antimicrobial activities of the synthesized compounds on selected bacteria (*S. typhi*, *E. coli*, *S. aureus*) and fungi strains (*A. niger*, *T. rubrum*, *C. abicans*) were comparable with streptomycin and fluconazole.The results showed that these compounds could serve as good raw materials for the manufacture of new drugs.

Keywords: Schiff base, hydrazones, synthesis, complexes, antimicrobial

*Corresponding author.
E-mail address: mynameisterungwa@gmail.com

1. Introduction

Hydrazones are organic compounds with the structure $R_1R_2C=N-NH_2$ (Al-Ajely, 2022; El-khlifi *et al.*, 2024). They are formed from the reaction between hydrazine, substituted hydrazine or hydrazides with aldehydes or ketones (Parveen and Kumar 2020). The reaction usually takes place under mild acidic conditions in solvents such as ethanol, methanol, or tetrahydrofuran (Singh *et al.*, 2013). Since the hydrazine molecule contains two amino groups, reactions with an excess of carbonyl compound result in two molecules of the carbonyl compound condensing with one molecule of the hydrazine (Reddy *et al.*, 2024; Settima *et al.*, 2024). The mechanism for the formation of hydrazones is shown in Scheme 1. Hydrazones have been extensively used as versatile ligands for the synthesis of biologically active complexes (Rajawat and Madhav, 2018) and as effective inhibitors of metallic corrosion (Ait Mansour *et al.*, 2025). Their versatility is due to their ability to form bidentate, tridentate and tetradentate ligands coupled with their interesting modes of coordination (Dikio *et al.*, 2017). A number of studies have shown that hydrazones complexes exhibit excellent biological activities such as antimicrobial, analgesic, anti-tubercular and anti-inflammatory properties (Khan *et al.*, 2024; Rajawat and Madhav, 2018). Studies have proven that the sensitivities and other biological properties demonstrated by hydrazones and their complexes depend on the structures and the ionic form they exist in solution (Eissa *et al.*, 2018). These studies have also proved that hydrazones metal complexes could serve as good raw materials for new drug design (Jankulovska *et al.*, 2017).

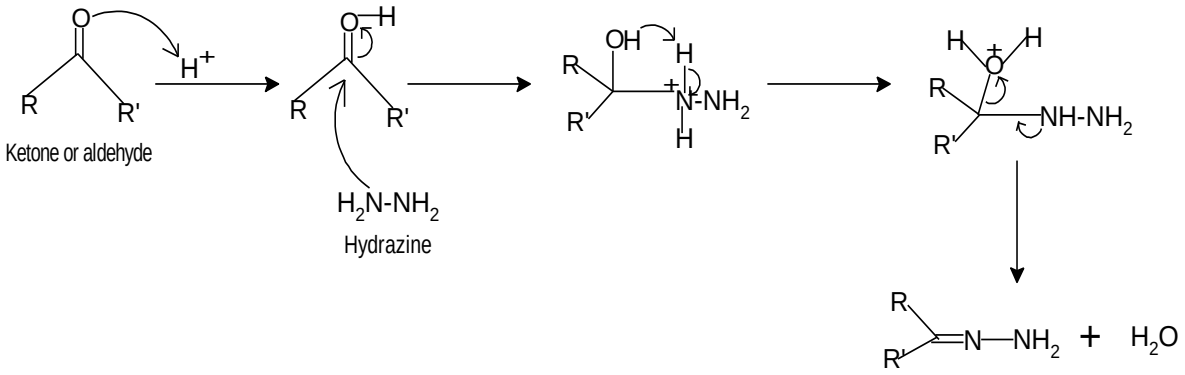

Scheme 1: Mechanism of hydrazone formation

In the aspect of analytical chemistry, hydrazones have been used as sensitive analytical reagents for the determination of trace amounts of metal ions in solutions (Jabeen 2022; Despaigne *et al.*, 2010). For example, 2-acetylfuran benzoyl hydrazone ligand have been successfully used for spectrophotometric determination of Cu(II) in aqueous medium (Basha 2017). Another very important area where hydrazones have found tremendous applications is in chemical industries. For example, fluorenone hydrazones derivatives and their complexes have been found to display satisfactory corrosion inhibition properties (Al-Jahdaly *et al.*, 2016; Lgaz *et al.*, 2019). Agricultural applications of

hydrazones have also been reported recently as they can be used as herbicides, insecticides and plant growth stimulants due to their physiological activity (Liu *et al*., 2010). Isonicotinic acid hydrazide (INH) has been used as a frontline drug for the treatment of tuberculosis. It has a great potency against *M. tuberculosis*. Studies have shown that complexes of isonicotinic acid hydrazone and its derivatives have excellent clinical properties. Therefore, incorporating metal ions to isatin-isonicotinylhydrazide is expected to produce hydrazone complexes with better antimicrobial properties.

2. Materials and methods

2.1. Laboratory materials

All the chemicals were bought from Sigma Aldrich and used as soon as they arrived without purification. Perkin Elmer FT-IR spectrophotometer (spectrum BX Model using spectrum version 5.3.1 software version), Perkin Elmer spectrophotometer UV-VIS double beam PC scanning spectrophotometer (UVD-2690), using UV-Winlab 2.8.5.04 software version, Magnetic stirrer, Gallenkemp melting point apparatus with digital thermometer, Jenway 4510 conductivity meter, UNISCOPE SM 9053 Laboratory oven, autoclave, aluminium foil paper, weighing balance, nose mask, meter rule, cotton wool, hand gloves, petri dishes, wire loop, paper disc.

2.2. Synthesis of the ligand, isatin-isonicotinyl hyrazide (ISINH)

A solution of isonicotinic acid hyrazide (0.01 mol, 1.371 g) in 50 cm^3 of ethanol was added to isatin (0.01mol, 1.521 g) in 50 cm^3. Three drops of glacial acetic acid were added to the mixture. The mixture was then stirred for 3 hours at room temperature using a magnetic stirrer. The resulting orange precipitate was collected after filtration. This precipitate was washed with ethanol and allowed to dry in a desiccator containing fused calcium chloride (Rao *et al*., 2010). The weight of the prepared precipitate was measured after drying. The equation for the reaction is as shown in Scheme 2.

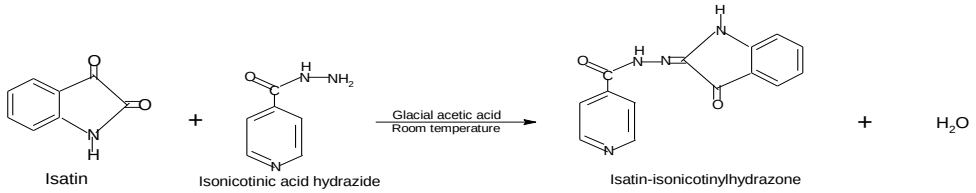

Scheme 2. Synthesis of the Schiff base ligand, isatin-isonicotinylhydrazone (ISINH)

2.3. Synthesis of the transition metal mixed ligand complexes

Ethanolic solutions of the metal salts in 30 cm^3 were added to the already prepared solution of the isatin-isonicotinylhydrazone (0.003 mol, 0.813 g). The mixture was stirred for 15 minutes before adding the thiophene as second ligand. The precipitates formed after three hours of stirring were

filtered, rinsed with ethanol and allowed to dry in a desiccator containing fused calcium chloride (Yorur-Goreci *et al*., 2016).

3. Results and discussion

3.1. Physical properties of ISINH and its mixed ligand complexes (Nature, Colour, Melting points and Conductivity)

The physical properties of the synthesized compounds (Nature, Colour, Melting points and Conductivity) were measured using physical observation, melting point apparatus and conductivity meter respectively. The compounds showed various physical properties as presented on Table 1, with the colour ranging from orange to reddish brown and ligand had lower melting point than the complexes.

Table 1. Physical properties of ISINH and its mixed ligand complexes

Compounds	Nature	Colour	Melting points (°C)	Conductivity (µs/cm)
ISINH	Powdery	Orange	287.6	0.03
$[Ni(ISINH)_2(T)_2]$	Powdery	Reddish brown	195.8	0.05
$[Cu(ISINH)_2(T)_2]$	Powdery	Brick red	206.2	0.10
$[Zn(ISINH)_2(T)_2]$	Powdery	Orange	238.1	0.07

The physical properties of the compounds showed on Table 1 that all the synthesized compounds were coloured and existed in powdery form indicating their polymeric nature. The compounds presented high melting points ranging from 195.8- 287.6 ºC and low conductivities in the range of 0.03-1.10 µs/cm. The high melting points displayed by the compounds could be as a result of the strong bonds formed between the ligand and the metal ions (Didarul *et al*., 2010). The sharp melting points obtained from the ligand and its mixed ligand complexes could be a confirmation of their purity (Fasina *et al*., 2016). The low conductivities displayed by the compounds indicated that the compounds were non-electrolytic (Al-Masoudi *et al*., 2023; Ogunniran *et al*., 2008). This means that the degree of dissociation of the compounds was low and therefore fewer ions were released into solution (Al-Masoudi *et al*., 2023).

3.2. Solubility data of ISINH and its mixed ligand complexes

The solubility of the synthesized compounds (ligand and complexes) in distilled water, ethanol, methanol, acetone and DMSO were determined at room temperature. As shown in Table 2, the compounds were soluble in acetone and DMSO and partially soluble in methanol, ethanol and distilled water. The solubility results showed that the ligands and the complexes were slightly soluble in water but exceedingly soluble in coordinating solvents like acetone and DMSO. This could be due to their

higher dipole moments of acetone (2.85 Debye) and DMSO (3.90 Debye) compared to 1.82, 1.72 and 1.68 Debye for water, ethanol and methanol respectively. The ligands and their mixed ligand complexes were all stable as they did not decompose while being stored in a desiccator for over four weeks.

Table 2. Solubility data of ISINH and its mixed ligand complexes

Compounds	Distilled water	Ethanol	Methanol	Acetone	DMSO
ISINH	SS	S	S	S	S
$[Ni(ISINH)_2(T)_2]$	SS	SS	SS	S	S
$[Cu(ISINH)_2(T)_2]$	SS	SS	SS	S	S
$[Zn(ISINH)_2(T)_2]$	IS	SS	S	S	S

3.3. Infrared spectrum of isatin-isonicotinylhydrazone (ISINH) amd its complexes

The FTIR spectral of the ligand and the complexes were run using KBr disc and the results presented from 350-4000 cm^{-1}. From Table 3, the results proved the ligand is bidentate with nitrogen and oxygen donor atoms. It coordinated the metal ion using its azomethine nitrogen and the lactone carbonyl (C=O) oxygen atom of the isatin moiety.

Table 3. Infrared spectra of ISINH and its mixed ligand complexes

Compounds	*v* (N-H)	*v* (C=O)	*v* (C=N)	*v* (C=C)	*v* (C-N)	*v* (C-O)	*v* (N-N)	*v* (M-N)	*v* (M-O)	*v* (M-S)
ISINH	3229s	1708s	1613s	1540	1460m	1296m	1073m	-	-	-
$[Ni (ISINH)_2(T)_2]$	3232s	1647s	1616s	1536	1460m	1339m	1106s	548w	463w	369w
$[Cu (ISINH)_2(T)_2]$	3227s	1687s	1611s	1536	1459m	1343m	1106s	561w	455w	348w
$[Zn (ISINH)_2(T)_2]$	3228s	1669s	1609s	1542	1461m	1339m	1110s	554w	441w	359w

The carbonyl group (C=O) vibration of the ISINH was seen as a strong band at 1708 cm^{-1}. The presence of the carbonyl vibrational band in the spectrum of the ligand and complexes shows that not all the carbonyl groups were involved in the formation of the Schiff base azomethine group. The strong absorption of the carbonyl (C=O) is due to the large change in dipole moment between the carbon and oxygen atom (Blagus *et al.*, 2010). This carbonyl group absorbed at this high frequency due to cyclization or ring strain associated with the ISINH molecule. From the spectra of the Ni(II), Cu(II) and Zn(II) complexes, the carbonyl (C=O) group absorbed strongly at 1647, 1687 and 1669 cm^{-1} respectively against 1708 cm^{-1} found in the ISINH spectrum. This shift in wavelength of absorption means that the carbonyl group coordinated to the metal ions. The azomethine group of these complexes was formed at 1609-1616 cm^{-1} against the 1613 cm^{-1} observed on the spectra of the ISINH suggesting coordination at this group. The shift in these frequencies is caused by changes in bond order and electron delocalization upon the chelate due to coordination. prominent vibrational band in

the spectrum of the ISINH at 3229 cm^{-1} was due to the *ν*(N-H). This group did not show any significant shift in the spectra of all the complexes which means it did not coordinate to the metal ions. This is because the carbon of the C=O group attached to this N-H group is electron withdrawing, thus reduces the ability of the N-H group to donate electrons to the metal ions. The additional weak bands in the spectra of the complexes at 548-561 cm^{-1} were due to M-N vibrations while the M-O were between 441-463 cm^{-1} (Sobola *et al*., 2014). Evidences of coordination of the thiophene sulphur atom to the metal atoms were seen from the M-S vibration bands that appeared at 348-369 cm^{-1}.

3.4. Electronic spectra of the complexes

The electronic measurements were used for assigning the stereochemistry of metal ions in the d-d transition peaks. The wavelengths of maximum absorptions displayed by the ligands along side with each of the complexes were obtained from their UV spectra. The UV spectra results displayed in Table 4 supported octahedral geometry for the complexes.

Table 4. UV spectra of ISINH and its metal- ISINH-T complexes

Compounds	Absorbance (nm)	Wavelength (nm)	Bands (cm^{-1})	Assignment	Geometry
ISINH	6.00	289	34,602	n- π*	
	1.32	326	30,674	π- π*	
$[Ni(ISINH)_2(T)_2]$	2.77	321	43,290	n- π*	
	2.38	362	27,624	π- π*	
	0.26	436	22,935	$^3A_{2g}(P)\rightarrow{}^3T_{1g}(F)$	Octahedral
	0.06	476	21,008	$^3A_{2g}(P)\rightarrow{}^3T_{1g}(P)$	Octahedral
$[Cu(ISINH)_2(T)_2]$	4.12	228	43,851	n- π*	
	3.48	311	32,154	π- π*	
	0.01	421	23,572	$^2E_g \rightarrow {}^2T_{2g}$	Octahedral
$[Zn(ISINH)_2(T)_2]$	3.27	238	42,016	n- π*	
	2.89	363	25,548	π- π*	
	0.05	459	21,786	L → M	Octahedral

The electronic absorption spectra are important to the study of metal complexes because they give additional information needed to elucidate the electronic transitions and the stereochemistry of compounds. The electronic absorption spectra of the Schiff base, ISINH displayed bands at 30,674 and 34,602 cm^{-1} attributed to π- π*and n- π* intra-ligand transitions respectively. The π- π* transitions are due to transitions in the azomethine group. The spectra of the complexes showed that, these bands were formed at higher absorption wave numbers proving that the ligand coordinated to the metal ions. The metal ions also showed some d-d transitions. The Ni(II) complex, $[Ni(ISINH)_2(T)_2]$ had its d-d transitions at 21,008 cm^{-1} and 22,935 cm^{-1} due to $^3A_{2g}$ (P)→ $^3T_{1g}$ (P)and $^3A_{2g}$ (P)→ $^3T_{1g}$(F) respectively. These transitions are in support of octahedral geometry for Ni(II) complex (Lakshmi *et al*., 2011). The copper (II) complex, $[Cu(ISINH)_2(T)_2]$ gave its d-d transitions at 23,572 cm^{-1}

assignable to $^2E_g \rightarrow {}^2T_{2g}$. The transitions presented by the copper complex are in line with octahedral geometry (Lawal *et al*., 2017; El Ati *et al*., 2022). The $[Zn(ISINH)_2(T)_2]$ complex did not produce d-d transitions due to the filled d^{10} configuration of the zinc hence expected to be white or colourless. However, the bands formed at 21,786 cm^{-1} and 25,548 cm^{-1} were due to ligand–metal charge transfer thus, it is coloured.

3.5. Thermal decomposition/ stability studies

The decomposition steps, temperatures and weight loss for all the synthesized compounds were recorded using a TGA. The results shown in Table 5 shows that the compounds decomposed in 3 to 4 steps with different weight loses the give the respective metal(II) oxides. The thermograms showing the decomposition pattern are shown in Figure 1, while the thermal behaviours curves are shown on Figure 2.

Table 5. Thermal decomposition steps and pattern / stability studies

Compounds	Steps	Temperature (°C)	Weight loss (%)	Residue (%)	Total weight loss
ISINH	I	25.5-291	2	19.8	80.2
	II	291-364	29.6		
	III	364-522	23.4		
$[Ni(ISINH)_2(T)_2]$	I	23.19-184	4	6.1	93.9
	II	182-336	33.2		
	III	336-397	55.8		
	IV	397-549	5		
$[Cu(ISINH)_2(T)_2]$	I	32.63-309	5.1	20.9	79.1
	II	309-55	74		
$[Zn(ISINH)_2(T)_2]$	I	26.36-200	6.1	12.2	82.2
	II	200-364	35.1		
	III	364-497	22.9		

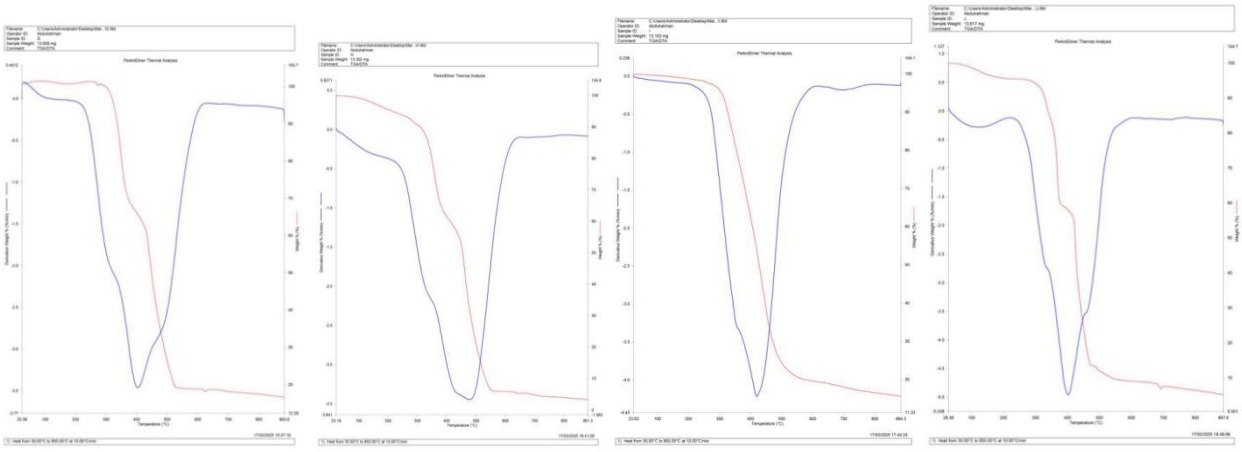

Ligand (L) Ni(II) complex Cu(II) complex Zn(II) complex

Fig. 1. TGA curve showing the decomposition pattern of the synthesized compounds

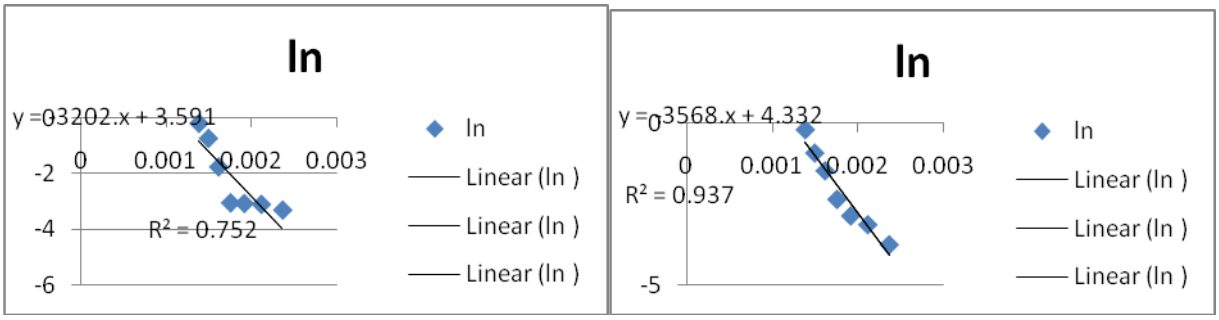

Plot for sample Zn complex

Plot for sample Ni complex

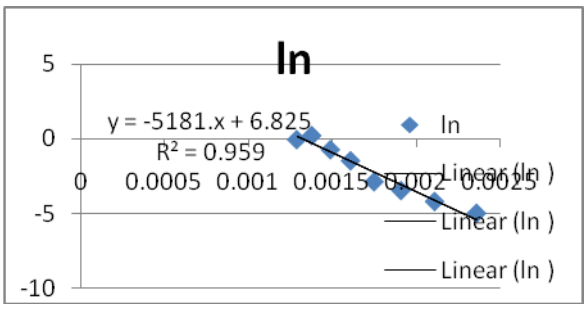

Plot of sample Cu complex

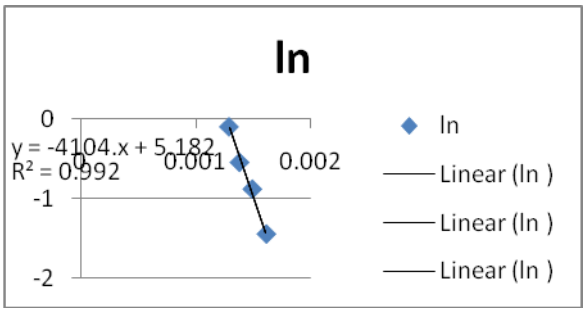

Plot of sample ligand

Fig. 2. Plots of ln $\frac{da}{dt}$ againt $\frac{1}{T}$ for each of the samples.

All the thermograms showed decrease in weight with increasing temperature which is an indication of fragmentation or disintegration. The ligand and all the complexes decomposed in two or more steps. The slow initial weight loss of 2 % in spectrum of the ligand from the temperature between 25.5-291 ^{o}C was due to loss of water molecules, ethanol solvent thiophene and other volatile compounds. This result showed that the ligand was stable up to 291^{o}C before decomposition began. The actual/major degradation occurred between 291 and 522 ^{o}C with weight loss of 53 %. The second degradation between 291-364 ^{o}C was attributed breakdown of hydrazone linkage and degradation of the isatin moiety, CO_2, CO and NH_3. The third degradation step between 364-522 ^{o}C with a weight loss of 23.4 % was due to further decomposition of the volatile aromatic ring and backbone. Beyond 522 ^{o}C, the ligand decomposed to form stable char or carbonate residue. The residue left in this case was due to ash, not metal oxides. Since thiophene is a small volatile organic molecule and evaporates quickly when heated, no char or residue of thiophene is left after decomposition of the complex. The total residue left after decomposition was 19.8 % while the total weight loss during decomposition process was 80.2 %. The decomposition pattern of the metal complexes showed the detachment of the ligand leaving behind the respective metal oxides as the final products.

The TGA-DTA curve of the Mn(II) complex showed that the complex underwent four decomposition steps. The first stage was the drying stage which occurred from 23.19 – 184 ^{o}C was slow. This stage was accompanied with a weight loss of 4 % due to loss of water molecules, ethanol, thiophene and other volatile compounds. The second, third and fourth decompositions occurred at 182-336 ^{o}C, 336-

397 and 347-549 ^{o}C respectively. These decompositions were accompanied by weight losses of 33.2, 55.8 and 5 % respectively. The first decomposition from 182-336 ^{o}C with a weight loss of 33.2% was due loss of isoniazid moiety (since it is thermally less stable compared to isatin). At this temperature range, the cleavage of –CONH-NH- or hydrazine like structure also occurs with the release of CO_2, H_2O, NH_3, CO etc. The decompositions between 336-397 and 347-549 ^{o}C were due to degradation of the indole structure of the isatin molecule with the release of gases such as CO and NO_2. Above the 549 ^{o}C, the Mn(II) complex decomposed to give char/residue of manganese(II) oxide MnO or Mn_3O_4. The nickel (II) complex showed only two decomposition steps; the first was in the drying stage (23.63-309 ^{o}C) with a weight loss of 5.1 %. The second step from 309-550 ^{o}C with a weight loss of 74 % %. This showed that the nickel (II) complex was stable up to 309 ^{o}C before it started decomposing. At temperature of above 550 ^{o}C, the compound decomposed to char leaving behind 20.9 % residue and formation of nickel (II) oxide, NiO. The drying stage of the Zn (II) occurred between 26.36 -288 ^{o}C with a weight loss of 6.1 %. The first decomposition stage occurred between 388-364 % with a weigh loss of 35.1 %. The second decomposition was between 364-497 ^{o}C. The total weight loss by the Zn(II) complex was 87.8 % and a 12.2 % residue of ZnO.

3.6. Kinetics and thermodynamic studies

The kinetics and the thermodynamic parameters for the formation were calculated from the TGA curve shown in Table 6. The kinetic and thermodynamic parameters on Table 6 shows that the processes were non spontaneous, endothermic and systems became more disordered as the complexes were formed. It was also observed that the Cu(II) complex is most resistant to decomposition or reaction hence more most kinetically stable.

Table 6. Results of thermodynamics and kinetic studies of ISINH and its mixed ligand complexes

Compounds	Regression equation	R^2	Ea (kJ/mol)	A (min^{-1})	Rate constant k (min^{-1})	ΔH (kJ/mol)	ΔG (kJ/mol)	ΔS (J/mol)
ISINH (L)	y= -4101.4x + 5.1826	0.9925	34.13	178.2	0.4190	28.50	198.65	-250.9
$[Ni(ISINH)_2(T)_2]$	Y = -3568.3x + 4.3322	0.9375	29.66	76.1	0.6675	23.40	220.43	-261.6
$[Cu(ISINH)_2(T)_2]$	Y = -5181.8x + 6.8256	0.9591	43.07	923.0	0.5218	37.31	204.93	-241.8
$[Zn(ISINH)_2(T)_2]$	Y = 3.202.2 x + 3.5913	0.7529	26.63	36.3	0.3215	21.00	177.07	-23.02

The ΔG gives the thermodynamic favourability and stability of a reaction or complex; lower or more negative ΔG values signify greater spontaneity and stability. The ΔG for the reactions were all positive and within the range of 177.5-220.43 kJ/mol. These positive values of ΔG shows that the all the

reactions were non spontaneous and therefore will need to be assisted to proceed. The assistance could be in form of grinding, refluxing, stirring, adding energy etc. The smaller the value of the ΔG, the more spontaneous the reaction proceeds and the less energy required to assist the reaction. Hence, the formation of the Zn complex (ΔG = 177.07 kJ/mol) will be more spontaneous and need less energy to proceed while that of the Ni(II) complex (ΔG = 220.43 kJ/mol) will be less spontaneous and less stable. Based on the ΔG values, the order of stability of the compounds is Zn> ISINH, Cu> Ni. The enthalpy change ΔH for the reactions were all positive (21.00-37.31 kJ/mol) implying that the reactions were endothermic. Thus these reactions will not emit/ liberate heat to the surrounding but rather will absorb heat from the environment. The entropy change (ΔS) for the reactions were all negative; -250.9. -261.6, -241.8 and -230.2 J/mol for ISINH, Ni, Cu and Zn complexes respectively. These negative of entropy values implied that the system became more disordered (complexes are more disordered than the reactants); hence the molecules may re-arrange themselves into a small structured form. Negative values of ΔS make the reactions/ process to be less thermodynamically favourable especially at higher temperatures because the TΔS becomes more positive leading to a less negative ΔG.

Kinetics studies

The activation energy (Ea) is the minimum amount of energy needed for a reaction to proceed/ occur. The activation energies obtained for the ISINH, Ni, Cu and Zn were 34.13, 29.66, 43.07 and 26.63 respectively. High activation energy means the reaction proceeds slowly, because more energy is needed to drive the reaction and the complex formed is less likely to decompose or react indicating greater kinetic stability. Thus the Cu(II) complex has the highest Ea (43.07 kJ/mol) while the Zn(II) complex has the lowest Ea (26.63 kJ/mol). This result showed that the Cu(II) complex is most resistant to decomposition or reaction hence more most kinetically stable. Contrary, the Zn(II) complex despite being thermodynamically stable has the lowest activation energy making it more reactive and hence less kinetically stable. Based on activation energy (Ea), the order of kinetic stability for the compounds is Cu > ISINH > Ni > Zn.

The rate constant shows the speed of a chemical reaction; higher rate constant implies faster reaction and more labile the complex formed but not necessarily more stable product. The smaller the rate constant, the slower the reaction and the more inert the complex formed. The rate constants for the formation of the ligand (ISINH), Ni, Cu and Zn complexes were 0.4190, 0.6675, 0.5218 and 0.3215/ min respectively. The results the rate constants showed that the Ni(II) complex had the highest rate constant (0.6675/min) which implies that the rate of formation of Ni complex will be fastest and may react/degrade faster. This agrees with its low Ea and low ΔG hence the Ni(II) complex is expected to

be more labile. On the other hand, the formation of the Zn(II) complex had the least rate constant (0.3215/min) which means that is the slowest reaction and more inert complex. Thus, the order if increasing inertness is Ni< Cu < ISINH < Zn.

The frequency factor (A) is the frequency of correctly oriented/effective collisions between reactants particles. These values can be used to predict the space or volume of space in the reaction molecule. The values of A obtained from the study were: 178.2, 76.1, 923.0 and 36.3 for the L, Ni, Cu and Zn complexes respectively. Based on the frequency factor values, the Cu(II) complex with the highest value (923.0) is expected to have the highest chances of successful collisions which helps to compensate for its Ea. The Zn(II) complex has the lowest collision which is in line with its slow rate of reaction. Since the value of the R^2 is close to unity, the reactions are said to be first order reactions.

3.7. Zones of inhibition (mm) for the $[M(ISINH)_2(T)_2]$

The zones of inhibitions on strains of bacteria (*S. Typhi*, *E. Coli* and *S. Aureus*) and fungi (*A. Niger*, *T. Rubrum* and *C. abican*) were determined by the disc diffusion method and the results shown on Table 7. The results showed that the complexes have better inhibition zones than the ligands. The complexes also displayed more antibacterial properties than fungal properties. The bar chat for the inhibitions is on Fig.3, while the plates used to measure the zones of inhibition are displayed in Figure 4 while

Table 7. Zones of inhibition for ISINH and its mixed ligand complexes (mm)

Compounds	*S. typhi*	*E. coli*	*S. aureus*	*A. niger*	*T. rubrum*	*C. abican*
ISINH	17	16	15	9	11	11
[Ni $(ISINH)_2(T)_2$]	28	29	26	17	24	23
[$Cu(ISINH)_2(T)_2$]	29	22	26	19	14	20
[Zn $(ISINH)_2(T)_2$]	31	28	32	12	16	24
Streptomycin/ Fluconazole	24	26	25	23	23	22

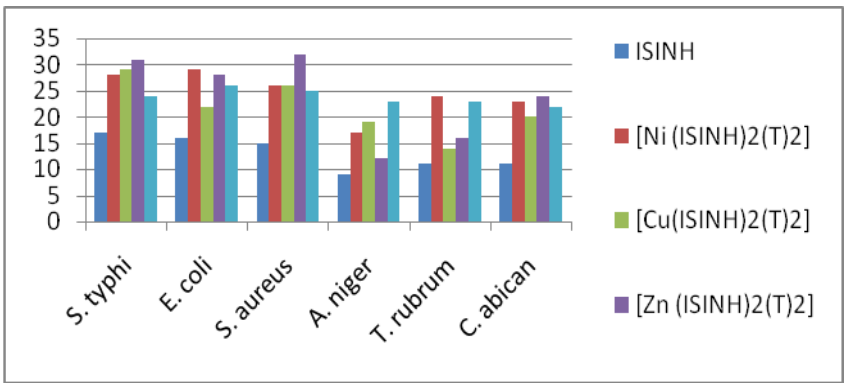

Fig. 3: Bar chat comparing the inhibition zones (vertical axis) of the ligand and its complexes for each microbe (horizontal axis).

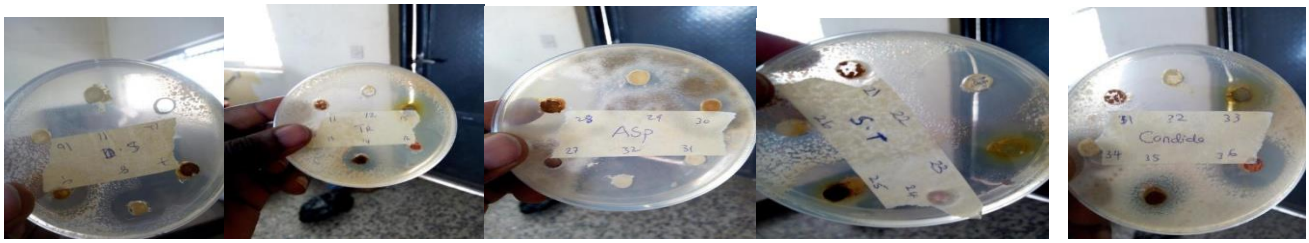

Fig. 4: Antimicrobial plates for measurement of inhibition zones.

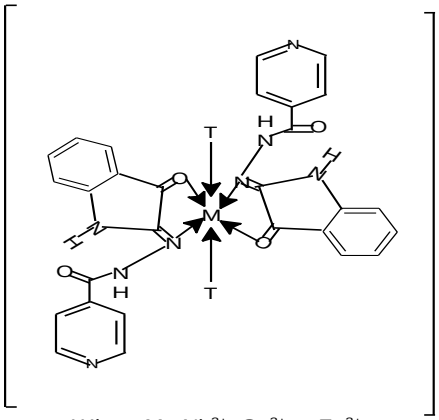

FIG. 5: Proposed structure for $[M(ISINH)_2(T)_2]$

Zones of inhibition measured for $[Ni(ISINH)_2(T)_2]$ against the bacteria strains were 26-29 mm. These zones were higher than the zones presented by streptomycin. On the other hand, its zones of inhibition against fungi were 17-29 mm, comparable with fluconazole. $[Cu(ISINH)_2(T)_2]$ and $[Zn(ISINH)_2(T)_2]$ presented higher zones of inhibition on the bacteria strains than that realized from streptomycin. However, their inhibition zones on fungi strains were lower than that of fluconazole. The complexes displayed far higher inhibition zones than the free ligands. This could be as a result of the combined effect of the two ligands which can be explained in terms of the Tweedy's chelation theory (Dharmaraj *et al*., 2001). As the complexes are formed, polarities of the metal ions are reduced to a greater extent due the overlapping of the ligand orbital and partial sharing of the positive charge of the metal ion with donor groups. Moreover, delocalization of the π-electrons over the whole chelate ring is increased and so does the lipophilicity of the complexes (Mounika *et al*., 2010). These properties now facilitate the penetration of the complexes across the membranes and DNA of the microbes leading to perturbation of the respiratory process of the cell and hinders the synthesis of proteins, leading to cessation of further growth of the microbes and its eventual death in extreme cases (Osipovna and Rauf 2023). The results of the MIC showed that they can be more effective in the treatment of bacterial infections than fungal infections. This indicates that these complexes can be used to treat diseases and infections caused by *E. coli*, *S. typhi* and *S. aureus*. They can also be used effectively for treatment of diseases caused by fungi strains such as *A. niger*, *T. rubrumand C. abicans*.

3.9. Minimum inhibitory concentrations of the $[M(ISINH)_2(T)_2]$

Minimum inhibitory concentration is the lowest concentration of an antimicrobial agent that can inhibit the growth of microorganisms but may or may not kill them. The results of the MIC on Table 8 showed that the compounds required smaller concentrations to inhibit the growth of the bacteria than fungi strains.

Table 8. Minimum inhibitory concentrations of ISINH and its mixed ligand complexes (mg/ml)

Compounds	*S. typhi*	*E. coli*	*S. aureus*	*A. niger*	*T. rubrum*	*C. abican*
ISINH	10.0	5.0	5.0	10.0	10.0	5.0
$[Ni(ISINH)_2(T)_2]$	5.0	2.5	2.5	5.0	2.5	2.5
$[Cu(ISINH)_2(T)_2]$	2.5	2.5	2.5	5.0	10.0	5.0
$[Zn(ISINH)_2(T)_2]$	2.5	5.0	2.5	10.0	5.0	5.0

The $[Ni(ISVN)_2(A)_2]$ inhibited the growth of both bacteria and fungi strains, it gave better effect on *S. typhi*, *S. aureus* and *A. niger* at a little concentration of 2.5 mg/ml. The $[Cu(ISVN)_2(A)_2]$ and $Zn[Mn(ISVN)_2(A)_2]$ had their MICs of 2.5 mg/ml and 5.0 mg/ml on the bacteria and fungi strains respectively. This result showed that it can inhibit bacteria even at a very low concentration but will require higher concentration to inhibit fungi strains. The $[Pt(ISIS)(T)_2]$ had a lower MIC of 5.0 mg/ml for all the bacterial strains studied. This result was lower than that obtained on the fungi strains (10 mg/ml). Thus the Platinum complex proved to be a better antibacterial agent that antifungal agent.

3.10. Minimum bactericidal and minimum fungicidal concentrations

Minimum bactericidal concentration (MBC) and minimum fungicidal concentration (MFC) are the smallest concentrations of an antimicrobial agent required to kill bacteria am fungi strains respectively. The results of the MBC and MFC on Table 9 showed that smaller concentrations were required to kill the bacteria than fungi.

Table 9. Results of minimum bactericidal and minimum fungicidal concentrations (mg/ml)

Compounds	*S. typhi*	*E. coli*	*S. aureus*	*A. niger*	*T. rubrum*	*C. abican*
ISINH	10.0	5.0	10.0	10.0	10.0	10.0
$[Ni(ISINH)_2(T)_2]$	5.0	2.5	2.5	10.0	5.0	2.5
$[Cu(ISINH)_2(T)_2]$	5.0	2.5	2.5	10.0	10.0	5.0
$[Zn(ISINH)_2(T)_2]$	2.5	10.0	5.0	10.0	10.0	5.0

The $[Ni(ISINH)_2(T)_2]$ complex presented an enhanced MBC and MFC in the range of 2.5-5.0 mg/ml on the studied microbial strains with the exception of *A. niger* which was 10 mg/ml. At 5.0 mg/ml, the

A. niger was fungistatic but grew unhindered at a concentration of 2.5 mg/ml. At concentration of 2.5 mg/ml, the $[Cu(ISINH)_2(T)_2]$ was able to prove its bactericidal strength against *E. coli* and *S. aureus* while its MFC was between 5.0-10.0 mg/ml. This proves that the $[Cu(ISINH)_2(T)_2]$ is more bactericidal than fungicidal. The *S. typhi* could not stand the effect of $[Zn(ISINH)_2(T)_2]$ even at a very low concentration of 2.5 mg/ml. For the rest of the micro organisms, the MBC and MFC were 5.0-10.0 mg/ml. The results showed that all the complexes were bactericidal and fungicidal at various concentrations. Since these compounds were found to be very effective on gram positive (*S. aureus*) and gram negative bacteria strains (*E. coli and S. typhyi*), they can be used as raw materials for the synthesis of broad spectrum antibiotics.

Conclusion

The synthesized compounds were found to be non electrolytic, stable to heat, non hygroscopic and monomeric in nature. The ligand ISINH was found to be bidendtate in nature with nitrogen and oxygen donor atoms. Octahedral geometry was proposed for the complexes. Thermal and kinetic studies proved that the decompositions of the compounds were non-spontaneous and endothermic and followed first order reaction. From the results of the antimicrobial analysis, the compounds are potential antimicrobial agents. The antibacterial strength displayed by the compounds showed they can be used as raw materials for synthesis of broad spectrum antibiotics.

Conflict of Interest

The authors declare that the research was conducted in the absence of any commercial or financial relationships that could be construed as a potential conflict of interest.

References

Ait Mansour A., Elmoutaouakil Ala Allah A., Lgaz H., Messali M., *et al*. (2025), Evaluation of N80 Carbon Steel Corrosion in 15 wt.% HCl Using Isatin-hydrazones: A Comprehensive Approach with Chemical, Electrochemical Techniques, and DFTB Calculations, *Journal of Molecular Structure*, 1321, Part 2, 139910, https://doi.org/10.1016/j.molstruc.2024.139910

Al-Ajely H. M. (2022). Green synthesis of new hydrazone derivatives. *International Journal of Applied Sciences and Technology*, 4(3), 531-535. http://dx.doi.org/10.47832/2717-8234.12.50

Al-Jahdaly B. A., Althagafi I. I., Abdallah M., Khairou K. S. & Ahmed S. A. (2016). Fluorenone hydrazone derivatives as efficient inhibitors of acidic and pitting corrosion of carbon steel. *Journal of Materials and Environmental Sciences*, 7(5), 1798-1809.

Al-Masoudi W. A., Mahmood H. Y., Jassim S. K., Al-Yassery M. N. (2023) Synthesis and antibacterial activities of Cu(II), Pd(II) and Co(II) complexes of Schiff base derived from L-methionine and 2-hydroxy-1-naphthaldehyde. *Advances in Bioresearch*, 14(2), 98-102. https://doi.org/10.15515/abr.0976-4585.14.2.98102

Basha S, V. (2017). Synthesis and characterization of 2-acetyl furan benzoyl hydrazone and its applications in the spectrophotometric determination of Cu(II). *Bioorganic and Inorganic Chemistry*, 1(3), 62-65.

Blagus A. Cincic D. Friscic T. Kaitner B. & Stilinovic V. (2010). Schiff bases derived fromhydroxyaryl aldehydes: molecular and crystal structure, tautomerism, quinoid effect, coordination compounds. *Macedonian Journal of Chemistry and Chemical Engineering*, 29(2), 117-138. https://doi.org/10.20450/mjcce.2010.159

Canpolat E., Aglamis A., Sahal H. & Kaya M. (2016). Some transition metal complexes of NO type Schiff base: preparation and characterization. *Cumhuriyet University Faculty of Science Science Journal*, 37(1), 65-73.

Despaigne A.A., Vieira L.F., Mendes I.C., Costa F.B., *et al*. (2010). Organotin(IV) complexes with 2-acetylpyridine benzoylhydrazones:Antimicrobial activity. *Journal of Brazilian Chemical Society*, 21(7): 1247-1257. https://doi.org/10.1590/S0103-50532010000700012

Dharmaraj N., Viswanathamurthi P. & Natarajan K. (2001). Ruthenium(II) complexes containing bidentate Schiff bases and their antifungal activity. *Transition Metal Chemistry*, 26(2), 105-109. https://doi.org/10.1023/A:1007132408648

Didarul A. C., Uddin C. M. & Hoque F. (2010). Dioxouranium(VI) complexes of some bivalent tridentate Schiff-base ligands containing ONS donor. *Setchiang Mai Journal of Science*, 37(3), 443-450.

Dikio C., W., Okoli B. J. & Mtunzi F. M. (2017). Synthesis of new anti-bacterial agents: hydrazide Schiff bases of vanadium acetylacetonate complexes. *Cogent Chemistry*, 3(1): 11-17. https://doi.org/10.1080/23312009.2017.1336864

Eissa H., Shaalan N., Mahde S. (2018). Synthesis, characterization, thermodynamic and biological activity studies for new complexes of some transition metals and zinc with Schiff's bases [2,5di(1-thi-ophen-2-yl-ethylidene)-hydrazine)1,3,4-`thia-diazole. *Organic and Medicinal Chemistry International Journal*, 5(2), 1-5. https://doi.org/10.19080/OMCIJ.2018.05.555659

El Ati R., Bouammali H., El Kodadi M., Yousfi E.B., Touzani R., Hammouti B. (2022). Study of the Catecholase Activity of new catalysts Based on Copper (II) and Heterocyclic Ligands, *Indonesian Journal of Science & Technology* 7(1), 1-18

El-khlifi A, Zouhair FZ, Al-Hadeethi MR, Lgaz H, Lee H-S, Salghi R, Hammouti B, Erramli H. (2024). Assessment of Hydrazone Derivatives for Enhanced Steel Corrosion Resistance in 15 wt.% HCl Environments: A Dual Experimental and Theoretical Perspective. *Molecules.* 29(5), 985. https://doi.org/10.3390/molecules29050985

Fasina T. M. Ejiah F. N., Oloba-Whenu O. A., Revaprasadu N. & Familoni O. B. (2016). Synthesis, characterization and structure activity relationship of Schiff bases derived from 2-aminophenol and substituted benzaldehydes. *FederalUniversity Wukari Trends in Science and Technology Journal*, 2(1), 252 -256.

Jabeen M. A. (2022). Comprehensive Review on analytical applications of hydrazone derivatives. *Journal of the Turkish Chemical Society Section A: Chemistry*, 9(3), 663–698 (2022). https://doi.org/10.18596/jotcsa.1020357

Jankulovska M. S., Dimova V. & Spirevska I. (2017) Investigation of acid-base properties of aromatic hydrazones in basic media at constant ionic strength. *Radiation Association Conference roceedings*, 2(1), 296-299. https://doi.org/10.21175/RadProc.2017.59

Khan T., Zehra S., Alvi A., Mishra N., Lawrence R., Joshi S., & Khan A. R. (2024). Synthesis, characterization, computational studies and antimicrobial activity evaluation of mixed ligand-metal complexes of selected thiosemicarbazones. *ChemistrySelect*, 9(10): e202400202 https://doi.org/10.1002/slct.202400202

Lgaz H., Chaouiki A., Al-Hadeethi M. R., Salghi R. (2019). Synthesis and evaluation of some new hydrazones as corrosion inhibitors for mild steel in acidic media. *Research on Chemical Intermediates*, 45(4), 1-18. https://doi.org/:10.1007/s11164-018-03730-y

Liu M. Wang Y., Wangyang W., Liu F., Cui Y., *et al*. (2010) Design, synthesis and insecticidal activities of phthalamidescontaining a hydrazone substructure. *Journal of Agricultural and Food Chemistry*, 58(9), 6858-6863. https://pubs.acs.org/doi/10.1021/jf1000919

Mounika K., Anupama B., Praghathi J. & Gyanakumari, C. (2010). Synthesis, characterization and biological activity of a Schiff base derived from 3-ethoxy salicyaldehyde and 2-amino benzoic acid and its transition metal complexes. *Journal of Scientific Research*, 2(3): 513-524. https://doi.org/10.3329/jsr.v2i3.4899

Ogunniran K.O., Ajanaku K.O. James O.O., *et al*. (2008). Cobalt(II) complexes of mixed antibiotics: synthesis, characterization, antimicrobial potentialand their effect on alkaline phosphate activities of selected rat tissues. *International Journal of Physical Science*, 3(8), 177-182.

Osipovna N. L., Rauf M. S. (2023). Mechanism of resistance of microorganisms to nickel compounds. *World Journal of Advanced Research and Reviews*, 17(02), 101–112. Doi:10.30574/wjarr.2023.17.2.0800

Parveen B. & Kumar, A. (2020). Synthesis and biological evaluation of new hydrazone. The *Pharma Innovation Journal*, 9(10), 506-512. https://doi.org/10.22271/tpi.2020.v9.i10g.5284

Rajawat A. K. & Madhav H. (2018) Study of transition metal complexes of hydrazones derived from different acid hydrazides: synthesis and characterization. *Indian Journal of Advances in Chemical Science*, 6(1): 8-16. https://doi.org/10.22607/IJACS.2018.601002

Rao K. V., Reddy S. S., Krishna B. S., *et al*. (2010) Synthesis of Schiff's bases in aqueous medium: a green alternative approach with effective mass yield and high reaction rates. *Green Chemistry Letters and Reviews*, 3(3), 217-223. https://doi.org/10.1080/17518251003716550

Shettima U. A., Ibrahim M. & Idongesit E. E. (2024). Synthesis, characterisation and antimicrobial studies of Schiff base ligand derived from salicylaldehyde and 2,4-dinitrophenyl hydrazine and its metals complexes. *Nigerian Research Journal of Chemical Sciences* 12(1), 219-234.

Singh V. P., Tiwari K., & Mishra M. (2013) Synthesis, spectral and thermal studies of some polymeric mixed ligand uracil- hydrazide complexes with transition metal ions, *Designed Monomers and Polymers*, 16(5), 456-464. https://doi.org/10.1080/15685551.2012.747164

Sobola A. O. Watkins G. M. & Brecht B. V. (2014). Synthesis, characterization and antimicrobial activity of copper(II) complexes of some ortho-substituted aniline Schiff bases; crystal structure of bis(2-methoxy-6-imino)methylphenol copper(II) complex. *South African Journal of Chemical Society*, 67(1), 45-51. https://doi.org/10.2298/JSC170913002S

Yorur-Goreci, C., Demir Z. & Altas N. (2016). Green synthesis of new amino acid schiff bases and their biological activities. *Journal of the Turkish Chemical Society* 3(3), 15-26. https://doi.org/10.18596/jotcsa.14900